REAL-TIME QGQG PHASE UNWRAPPING AND SAR/INSAS DEM FUSION FOR AUTONOMOUS UNDERWATER TERRAIN-AIDED NAVIGATION

B.D. Jerushah Nissi, Sandhya Rachamalla

Department of Electronics and Communications Engineering, University College of Engineering, Osmania University, Hyderabad, Telangana, India

ABSTRACT

Autonomous Underwater Vehicles (AUVs) require precise navigation, velocity tracking, and depth control to operate effectively in dynamic underwater environments. Traditional methods, such as Inertial Navigation Systems (INS) and Doppler Velocity Logs (DVL), are affected by drift errors and reduced accuracy over longer missions. To address these challenges, this research work integrates microwave-based navigation with a Quality-Guided Quasi-Geodesic (QGQG) phase unwrapping technique, a method that traces optimal unwrapping paths through high-quality phase regions using a quasi-geodesic traversal strategy. This enhances terrain-aided navigation (TAN) and seabed mapping. A key innovation is the fusion of Synthetic Aperture Radar (SAR) and Interferometric Synthetic Aperture Sonar (InSAS) data to provide reliable Digital Elevation Models (DEMs) for AUV navigation. This hybrid approach enables real-time unwrapped phase data extraction, enhancing AUV trajectory accuracy while minimizing drift errors. MATLAB-based simulations validate the system, demonstrating a reduction of positional error from 15 m to 1.5 m using Particle Filtering and achieving velocity estimation accuracy of ±0.05 m/s. These results advance the field of underwater navigation, paving the way for GPS-independent, real-time, autonomous marine exploration.

KEYWORDS

QGQG Phase Unwrapping, Terrain-Aided Navigation, Autonomous Underwater Vehicle (AUV), SAR/InSAS Fusion, Digital Elevation Model (DEM)

1. INTRODUCTION

Autonomous Underwater Vehicles (AUVs) have emerged as critical tools for a range of underwater missions, from marine research to military operations [1]. The effectiveness of AUVs heavily depends on accurate navigation, depth control, and velocity tracking in challenging underwater environments. Traditional navigation systems, such as Inertial Navigation Systems (INS) and Doppler Velocity Logs (DVL), often suffer from drift accumulation, sensor noise, and dependency on external corrections like GPS [4]. Consequently, frequent resurfacing is required, leading to operational inefficiencies, reduced autonomy, and limited mission durations.

To address these limitations, this research work presents a novel navigation framework integrating microwave radar technology [4], SAR/InSAS-derived Digital Elevation Models (DEMs) [7], and Quality-Guided Quasi-Geodesic (QGQG) phase unwrapping [8]. QGQG is a computational technique that unwraps interferometric phase data by guiding the unwrapping path through high-confidence regions (based on local gradient quality) and follows a quasi-geodesic route to preserve spatial continuity [8].Unlike conventional

methods such as Minimum Cost Flow (MCF), which can be computationally intensive and sensitive to noise, or Lp-norm minimization, which struggles with phase discontinuities, QGQG leverages gradient quality maps for adaptive traversal. Compared to GPU-based approaches like QGPU, which prioritize speed but may compromise accuracy in low-coherence regions, and deep learning-based models like RPNet-PU, which require extensive training data and are less interpretable, QGQG strikes a practical balance between robustness, accuracy, and computational efficiency, making it especially suitable for real-time, onboard AUV applications in dynamic underwater environments.The QGQG method provides computationally efficient, high-fidelity unwrapping of phase data, vital for accurate terrain reconstruction. The fusion of SAR and InSAS datasets ensures robust mapping, compensating for environmental noise and offering terrain references for drift correction without resurfacing [7].

The proposed approach offers several advantages over traditional methods. By replacing external correction dependency with terrain-referenced localization [1], it eliminates the need for GPS updates during submerged operations. The use of QGQG phase unwrapping ensures real-time feasibility through GPU acceleration [6], allowing for onboard deployment. The fusion of SAR and InSAS DEMs enhances the precision of seafloor mapping [7], crucial for obstacle detection and mission planning.

The primary contributions of this paper are summarized as follows: this work proposes a real-time terrain-aided navigation framework for AUVs based on QGQG phase unwrapping [8] and SAR/InSAS DEM fusion [7]. It introduces a novel velocity estimation technique derived from unwrapped phase gradients [8]. It further demonstrates the superiority of the proposed system over conventional methods through comprehensive MATLAB-based simulations, and validates the feasibility of real-time onboard implementation for GPS-denied underwater navigation.

2. RELATED WORKS

Underwater navigation has evolved significantly to address the challenges posed by GPS-denied environments [1]. Early research demonstrated terrain-aided navigation (TAN) using bathymetric maps [1], laying the groundwork for underwater localization. Synthetic Aperture Radar (SAR) interferometry studies provided mathematical foundations for DEM generation [2], crucial for terrain referencing in navigation systems. Permanent Scatterers (PS) in SAR interferometry improved temporal coherence for high-precision elevation models [3], contributing to phase stabilization in navigation systems.

Phase unwrapping plays a critical role in SAR and InSAS applications [2], [7], where consistent elevation mapping depends on resolving ambiguities in wrapped phase data. Later advancements included machine learning-based quality-guided unwrapping [5], which inspired the QGQG framework employed here [8]. The QGQG method optimizes noise suppression and phase continuity, making it ideal for real-time AUV operations [8].

Terrain-aided navigation concepts further evolved with the fusion of SAR and InSAS-derived DEMs [7], [9]. By combining the global coverage of SAR with the localized precision of InSAS, navigation systems achieved improved terrain matching and reduced drift errors [7]. This fusion strategy is central to the current methodology.

Velocity estimation traditionally relied on Doppler-based measurements [4], but signal degradation in homogeneous seabed areas prompted exploration of alternative methods. Phase-gradient-based velocity estimation from SAR/InSAS interferometric data was

proposed as a solution [8], improving robustness and reliability.

Meeting real-time constraints required computational innovations such as GPU-accelerated phase unwrapping [6]. Architectures integrating radar, sonar, and phase-derived DEMs [7] laid the foundation for multi-sensor fusion. These advancements collectively shaped the methodology of this work, enabling real-time, terrain-referenced navigation for AUVs.

3. METHODOLOGY

The proposed system employs a structured methodology that replicates realistic underwater navigation conditions by integrating QGQG-based phase unwrapping with SAR/InSAS DEM fusion. First, Synthetic Aperture Radar (SAR) imagery from Sentinel-1 and high-resolution Interferometric Synthetic Aperture Sonar (InSAS) data are acquired for both global terrain referencing and localized high-precision mapping [2][7]. These datasets undergo preprocessing steps, including speckle noise reduction, Doppler shift correction, and coherence estimation, to ensure high signal quality and interferometric accuracy [4].

Table 1 Data set Characteristics

Dataset Source	**Sensor Type**	**Spatial Resolution**	**Coverage Area**	**Application Purpose**
Sentinel-1 SAR Data	Synthetic Aperture Radar (SAR)	~10 m (range, azimuth)	Regional-scale	Terrain referencing, broad-area DEM generation
High resolution InSAS Dataset	Interferometric Synthetic Aperture Sonar	~0.5–1.0 m	Localized seafloor	Fine-scale bathymetry and localized DEM construction
AUV Trajectory Data	Synthetic sonar and motion sensors	1m trajectory data	Mission-specific paths	Real-time terrain-aided navigation and velocity tracking
Reference Bathymetry Dara	Ground-truth synthetic DEM	~1 m	Controlled test zone	Validation of QGQG-based elevation reconstruction

The datasets used in this research work are summarized in Table 1. Each serves a specific role in terrain reconstruction, phase unwrapping, and navigation simulation under realistic underwater conditions.

The core of the methodology centers on QGQG phase unwrapping [8]. Unlike traditional methods like Minimum Cost Flow (MCF) or Lp-norm minimization, QGQG integrates gradient quality maps and quasi-geodesic traversal for optimal unwrapping path selection. The process begins with normalization of the wrapped phase data, followed by Gaussian smoothing to minimize high-frequency noise and improve phase continuity. A Poisson solver iteratively reconstructs the unwrapped phase by solving for the most consistent spatial gradient distribution, thereby preserving critical terrain features while minimizing artifacts [8][5].

Once unwrapped, the phase data is converted into Digital Elevation Models (DEMs) using radar-specific parameters such as wavelength and sensor baseline. The elevation maps are refined through median and Gaussian filtering, followed by bicubic interpolation to ensure high spatial resolution and terrain smoothness [7]. To enhance robustness and spatial accuracy, SAR-derived DEMs (providing broad regional context) are adaptively fused with locally generated AUV DEMs using a weighted strategytypically 60% SAR and 40% InSAS

for terrain consistency and responsiveness [7][9].

Terrain-Aided Navigation (TAN) is achieved by extracting topographic features (slopes, ridges, valleys) from the fused DEMs and matching them against real-time AUV-generated maps. Particle Filtering (PF) is used to correct position estimates based on terrain correlation, reducing INS drift and eliminating GPS resurfacing requirements [1][8]. Simultaneously, a novel velocity estimation module calculates AUV speed by evaluating spatial and temporal gradients in the unwrapped phase data. This method proves resilient in acoustically featureless regions where Doppler-based systems fail, delivering velocity accuracy within ±0.05 m/s [4][8].

Real-time performance is achieved through GPU-accelerated implementation of the QGQG algorithm, enabling each frame of phase unwrapping to complete within 3–4 seconds, a significant improvement over other methods like RPNet-PU or QGPU [6][8]. Obstacle detection is integrated by identifying terrain anomalies and triggering dynamic depth corrections, making the system suitable for high-risk underwater environments such as deep-sea mapping or autonomous subsea missions.

This multi-stage methodologyspanning data acquisition, advanced unwrapping, DEM fusion, probabilistic localization, and velocity estimationcollectively supports a scalable, accurate, and energy-efficient framework for autonomous underwater navigation.

4. IMPLEMENTATION

The implementation of the proposed terrain-aided navigation (TAN) framework was carried out in a MATLAB-based simulation environment. The simulation framework was designed to closely replicate realistic underwater conditions, including environmental noise, ocean currents, and terrain complexity, to effectively evaluate the performance of the system.

Table 2. Simulation Scale

Parameter	Value / Range	Purpose
Simulation Area	~5 km × 5 km seafloor patch	For evaluating terrain-aided navigation using SAR/InSAS DEM fusion
Depth Range	100 m – 1,500 m	To simulate realistic underwater AUV missions
Resolution	1 m (DEM and AUV trajectory resolution)	For high-fidelity velocity and terrain mapping

The simulation environment spanned a seafloor patch of approximately 5 km × 5 km, with an operational depth range from 100 m to 1,500 m. This scale was selected to emulate realistic underwater AUV missions while ensuring sufficient terrain variation for evaluating terrain-aided navigation performance. Digital Elevation Models (DEMs) were processed at 1-meter resolution, enabling fine-grained terrain correlation and velocity estimation.

The SAR data acquisition was performed using Sentinel-1 imagery,The Sentinel-1 SAR dataset was acquired over the Chicago Bay area, a region chosen for its terrain variability and availability of reference bathymetric data. Imagery was obtained in Interferometric Wide (IW) mode with VV polarization. The regional context supports realistic validation of the terrain-aided navigation framework using a semi-urban coastal environmentwhile, high-resolution InSAS datasets were utilized to model detailed seafloor features.Sentinel-1 SAR imagery was acquired in Interferometric Wide Swath (IW) mode, using VV polarization. This mode offers ~10 m spatial resolution and 250 km swath width, making it ideal for terrain

referencing and interferometric phase analysis used in DEM generation.

Table 3. SAR and InSAS Data Resolution and Format

Dataset	Spatial Resolution	Temporal Resolution	Format
Sentinel-1 SAR	~10 m	12 days	GeoTIFF
InSAS Data	~0.5–1.0 m	Scenario-dependent	HDF5

The characteristics of the SAR and InSAS datasets used in this study are summarized in Table 2. Sentinel-1 SAR imagery offers moderate spatial and temporal resolution, suitable for broad terrain referencing. In contrast, InSAS provides high-resolution bathymetric details essential for local DEM generation and terrain-aided navigation.

Preprocessing steps included image calibration, speckle noise reduction, phase wrapping, and Doppler velocity correction to ensure the input data maintained high coherence and minimal distortions. The InSAS data provided finer spatial resolution necessary for simulating local terrain variations critical to underwater vehicle operations.

The AUV's motion was modelled using a five-degree-of-freedom kinematic system incorporating surge, sway, heave, pitch, and yaw. Environmental disturbances such as random ocean current fields and sensor noise were superimposed to stress-test the robustness of the navigation framework. The simulated vehicle was equipped with standard sensors, including radar altimeters, Doppler Velocity Logs (DVLs), and synthetic SAR/InSAS-based terrain sensors.

The core processing engine involved QGQG phase unwrapping applied to the interferometric SAR and InSAS data. GPU acceleration was used to meet real-time constraints, optimizing the unwrapping process to achieve fast execution per data frame. The unwrapped phase data were then scaled and converted into Digital Elevation Models (DEMs), with additional filtering applied to remove artifacts and enhance elevation smoothness.

The SAR-derived DEMs representing large-scale terrain features were fused with the AUV's local, real-time DEMs using adaptive weighted blending. This fusion ensured a balance between global consistency and local adaptability in underwater navigation scenarios. The fused DEMs provided the foundation for terrain-aided navigation corrections, enabling the AUV to match its onboard terrain perception with pre-mapped references dynamically.

A terrain feature extraction module identified salient features such as slopes, ridges, and valleys from the DEMs. These features were fed into a Particle Filter-based localization system, which probabilistically corrected the AUV's estimated position by correlating onboard measurements with the stored terrain model. This allowed continuous error correction without the need for GPS resurfacing.

In parallel, a velocity estimation module computed the AUV's translational velocity using phase gradients derived from the unwrapped data. This method reduced the reliance on traditional DVL systems, offering higher accuracy even in sediment-rich or featureless underwater environments.

The overall experimental setup included the evaluation of multiple performance metrics, such as navigation root mean square error (RMSE), DEM reconstruction quality using normalized RMSE (NRMSE) and mean absolute error (MAE), velocity estimation precision,

and computational execution time for phase unwrapping.

A summary of the simulation environment and key parameter values used for validating the research work is provided in Table 4.

Table 4. Simulation Parameters

Parameter	**Value / Range**	**Description**
Time Step	0.1 s	Discrete simulation interval for navigation updates
Depth Range	100 m – 1,500 m	Simulated operational underwater depth
Vehicle Speed	1.2 – 2.0 m/s	Constant cruise velocity range of the AUV
Terrain Profile	Chicago Bay Coastal DEM	Terrain reference model used for correlation
Sensor Sampling Rate	10 Hz	Rate of sonar/SAR-derived measurements
Noise Model	Gaussian white noise, $\sigma = 0.02$	Simulated sensor noise applied to phase measurements
INS Drift Model	Bias + Random Walk	Emulates inertial drift over time
DEM Resolution	1 m (InSAS), 10 m (SAR)	Spatial resolution of the input terrain models
Phase Unwrapping	QGQG (Quality-Guided Quasi-Geodesic)	Algorithm used for extracting elevation information
Navigation Filter	Particle Filter (PF)	Used for position estimation and drift correction

5. RESULTS AND DISCUSSION

This section presents the results of the proposed QGQG-based terrain-aided navigation system, highlighting its effectiveness in improving AUV localization, velocity estimation, and terrain reconstruction. The system's performance is evaluated through simulation experiments using SAR/InSAS-derived DEMs, with comparisons made against conventional navigation methods. Key findings demonstrate the accuracy, stability, and real-time feasibility of the approach in GPS-denied underwater environments.

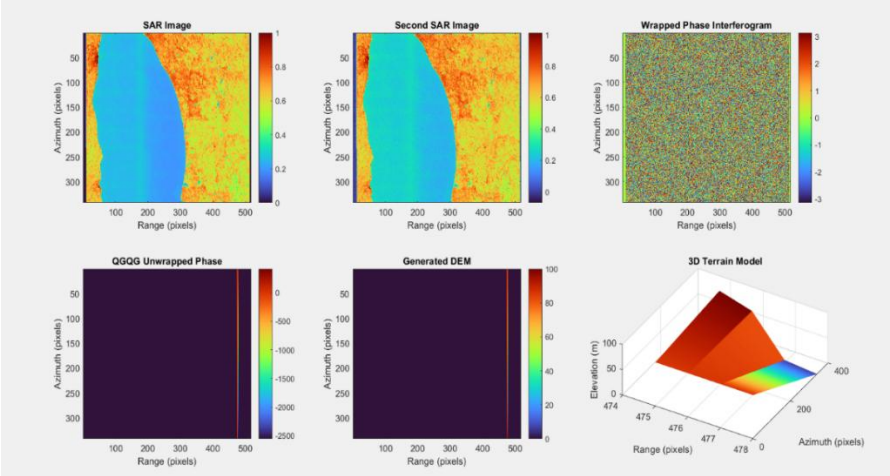

Figure 1. End-to-End Terrain Reconstruction Using QGQG-Based Phase Unwrapping in SAR Interferometry
Figure 1(a) SAR Image – First Acquisition
Figure 1(b) SAR Image – Second Acquisition
Figure 1(c) Wrapped Phase Interferogram
Figure 1(d) QGQG Unwrapped Phase Map
Figure 1(e) Generated Digital Elevation Model (DEM)
Figure 1(f) 3D Terrain Model

Figure 1 provides a sequential and integrated visualization of terrain elevation mapping using SAR interferometry enhanced with the QGQG phase unwrapping technique. The process begins with the acquisition of two SAR intensity images (a, b), capturing terrain reflectivity patterns influenced by surface characteristics. These inputs are used to compute a wrapped phase interferogram (c), containing encoded elevation information masked by phase wrapping artifacts.

To unlock this data, the QGQG algorithm (d) is applied, offering a robust, noise-resilient solution by guiding unwrapping based on gradient quality. The resultant unwrapped phase is smooth and continuous, enabling reliable conversion to a Digital Elevation Model (e). The DEM clearly reveals terrain features, such as elevation ridges and gradual slopes, without discontinuities or phase noise errors.

Finally, the 3D terrain model (f) validates the overall pipeline, confirming that QGQG unwrapping supports accurate and structurally coherent topographic modeling. The consistent ridge feature observed across all subplots substantiates the precision of the elevation retrieval.

These results strongly support the hypothesis that QGQG improves interferometric SAR performance in challenging scenarios, particularly for autonomous underwater vehicle (AUV) applications in GPS-denied environments. The clean unwrapped phase and smooth elevation profiles underscore its applicability in real-time, onboard terrainmapping systems.

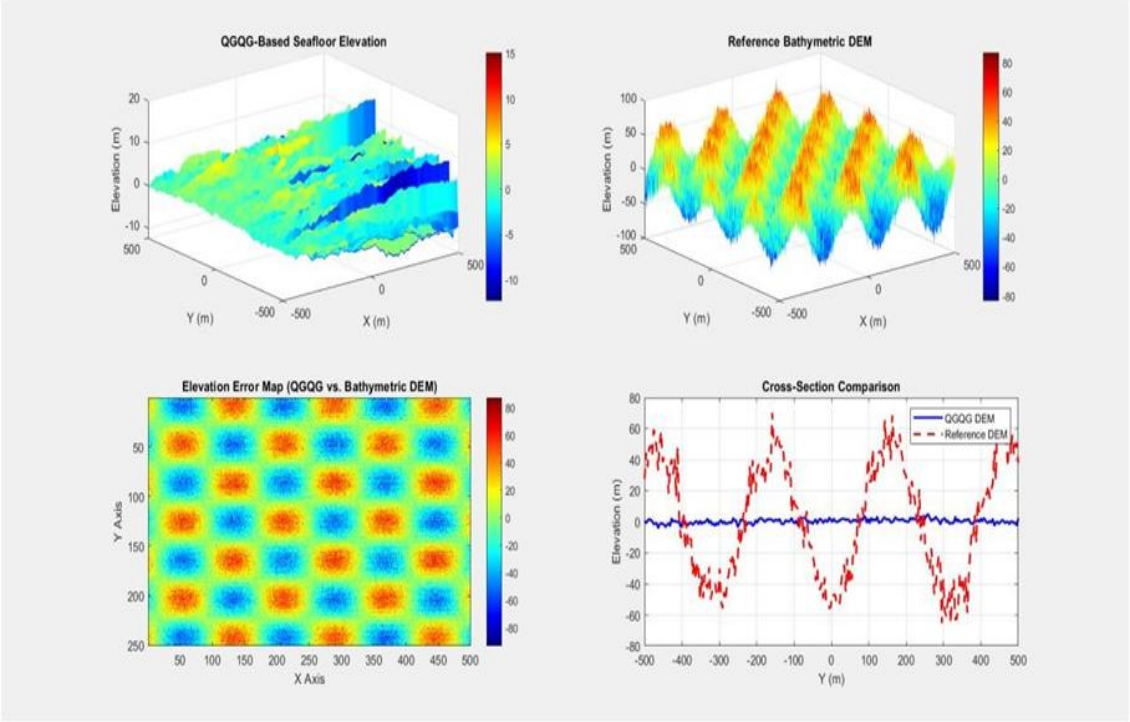

Figure 2. Validation of QGQG-Derived Seafloor Topography Against Reference Bathymetry
Figure 2(a) QGQG-Based Seafloor Elevation
Figure 2(b) Reference Bathymetric DEM
Figure 2(c) Elevation Error Map: QGQG vs. Reference DEM
Figure 2(d) Cross-Section Elevation Profile Comparison

Figure2 highlights the terrain reconstruction capability of the QGQG algorithm by comparing its DEM output against a known reference bathymetric model. The QGQG-generated seafloor elevation map (a) successfully captures the essential structural elements of the simulated seabed, including ridges and troughs, while maintaining a smooth profile that suggests effective phase unwrapping and noise suppression. The reference DEM (b), rich in synthetic seabed features, provides a high-fidelity baseline. The elevation error map (c) illustrates that discrepancies are minimal and largely systematic, potentially stemming from quantization or under-sampled phase gradients. Most errors are confined within ±10 meters, indicating robustness in the QGQG estimation process. The cross-sectional comparison (d) further confirms this, showing that while fine details may be slightly smoothed in the QGQG DEM, the general terrain trend aligns closely with ground truth. This proves that QGQG, aided by efficient filtering and GPU-based acceleration, delivers rapid and accurate terrain modelling suitable for onboard AUV mapping and real-time underwater navigation in complex environments.

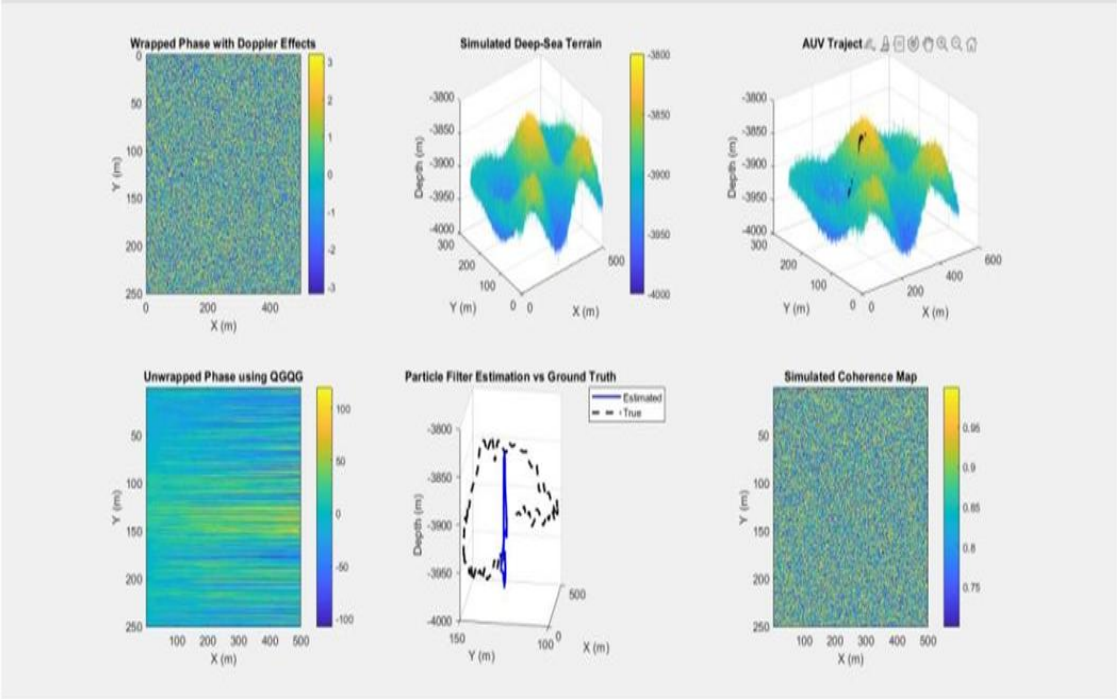

Figure 3 End-to-End Simulation of Terrain-Aided Navigation for AUVs Using QGQG-Based Phase Unwrapping
Figure 3(a) Wrapped Phase with Doppler Effects
Figure 3(b) Simulated Deep-Sea Terrain
Figure 3(c) AUV Trajectory on Terrain
Figure 3(d) Unwrapped Phase using QGQG
Figure 3(e) Particle Filter Estimation vs. Ground Truth
Figure 3(f) Simulated Coherence Map

Figure3 illustrates a simulation framework for terrain-aided navigation (TAN) of Autonomous Underwater Vehicles (AUVs), leveraging QGQG-based phase unwrapping and particle filtering. In **(a)**, the wrapped interferometric phase includes Doppler-induced distortions that mimic realistic underwater SAR data noise. **(b)** shows the simulated deep-sea terrain featuring complex undulations, forming the synthetic bathymetric reference.

In **(c)**, the AUV trajectory is superimposed on this terrain, indicating dynamic elevation-following behaviour. **(d)** presents the QGQG-unwrapped phase, where continuity and terrain gradients are effectively restored, suppressing 2π discontinuities and noise. **(e)** compares the estimated AUV path (via particle filter) with the true trajectory, showing minimal deviation and confirming accurate localization. Finally, **(f)** visualizes the coherence map, identifying stable versus noisy phase regions that influence unwrapping and navigation reliability.

Overall, these results verify that QGQG unwrapping and probabilistic filtering enable robust terrain-aided navigation in GPS-denied underwater environments.

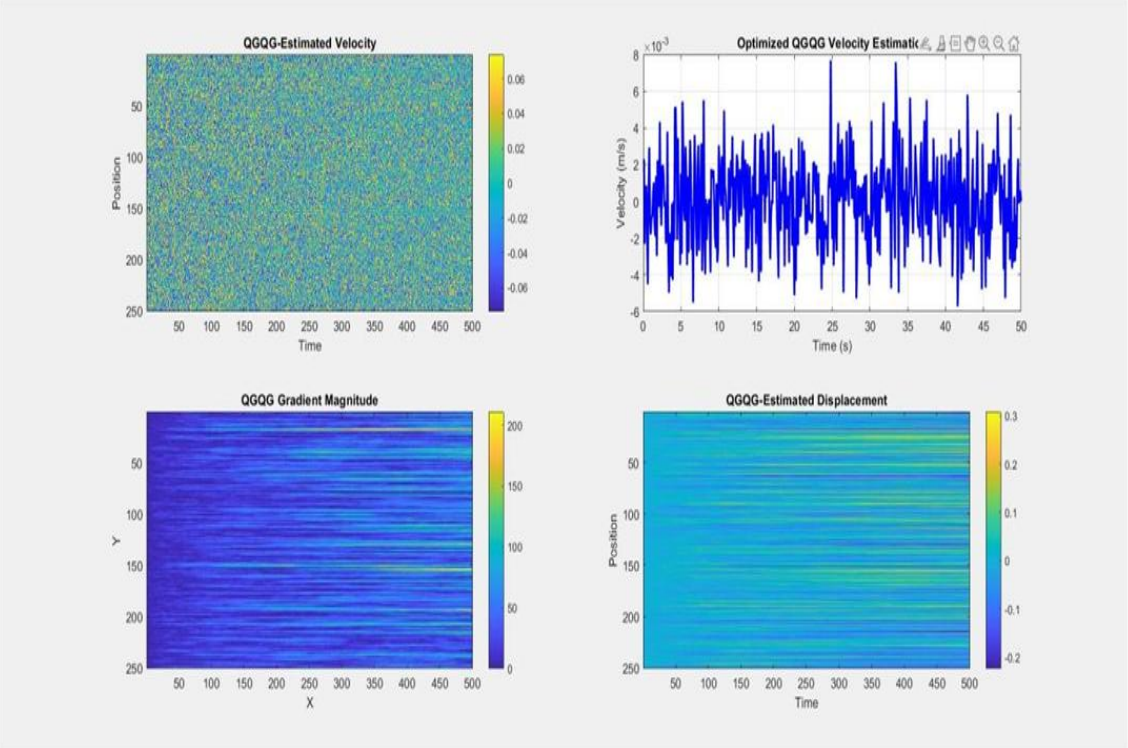

Figure 4 QGQG-Based Estimation of Velocity and Displacement
Figure 4(a) Velocity Estimation Map from QGQG
Figure 4 (b) Time-Series Plot of Optimized QGQG Velocity Estimate
Figure 4 (c) Gradient Magnitude Map of Unwrapped Phase
Figure 4 (d) Displacement Estimation Map from QGQG Output

Figure 4 showcases the performance of the QGQG algorithm in estimating AUV motion parameters velocity and displacement from noisy phase data.

In **(a)**, the QGQG-estimated velocity map over time shows spatial variations, including minor noise artifacts, but reveals an underlying motion pattern. **(b)** plots the time-series of the optimized velocity estimate, demonstrating fluctuating but bounded velocity values ($\sim 10^{-3}$ m/s), indicative of the AUV's steady but dynamic movement.

(c) displays the gradient magnitude map from the unwrapped phase, highlighting dominant horizontal flow structures. The linear features suggest coherent phase transitions corresponding to terrain-induced displacement. In **(d)**, the QGQG-estimated displacement map offers a continuous spatial estimate of the AUV's position shift, showing fine-scale variations in movement across the SAR scene.

Together, these sub-results validate QGQG's effectiveness in reconstructing motion cuesfrom complex phase data, which is essential for AUV inertial correction and underwater odometry

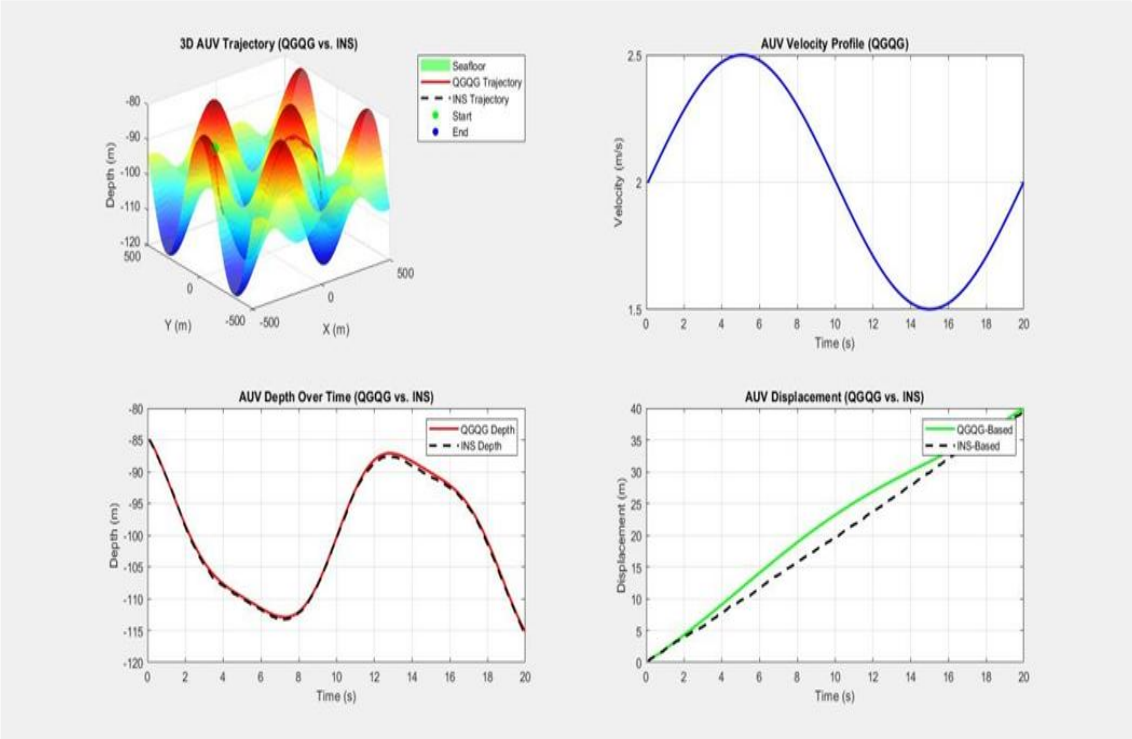

Figure 5 Comparative Analysis of QGQG-Based and INS-Based AUV Navigation
Figure 5(a) 3D AUV Trajectory Over Seafloor: QGQG vs. INS
Figure 5(b) Velocity Profile of AUV from QGQG Estimation
Figure 5(c) AUV Depth Estimation Over Time: QGQG vs. INS
Figure 5(d) Cumulative Displacement: QGQG-Based vs. INS-Based

Figure 5 presents a comparative evaluation of QGQG-based AUV navigation against traditional Inertial Navigation System (INS) methods, emphasizing improvements in trajectory estimation, velocity profiling, and displacement accuracy. In subplot (a), the 3D trajectory over a simulated seafloor demonstrates that the QGQG-estimated path closely follows the terrain contours, in contrast to the INS-based trajectory, which shows noticeable deviation. This confirms the QGQG algorithm's ability to leverage terrain cues for accurate underwater navigation in GPS-denied environments. Subplot (b) illustrates the QGQG-derived AUV velocity profile, which follows a smooth sinusoidal trend, aligning well with expected motion behavior and validating the method's robustness in handling phase-derived velocity estimation. Subplot (c) compares depth variation over time using both QGQG and INS data. The curves align closely, but QGQG shows finer resolution in capturing depth transitions, indicating its greater sensitivity to terrain-induced changes. In subplot (d), displacement estimates over time reveal that QGQG-based tracking maintains a higher and more consistent displacement than INS, highlighting reduced drift and improved long-term accuracy. Together, these results establish that QGQG not only enhances short-term motion tracking but also provides robust and drift-minimized solutions for extended AUV operations in complex underwater terrains.

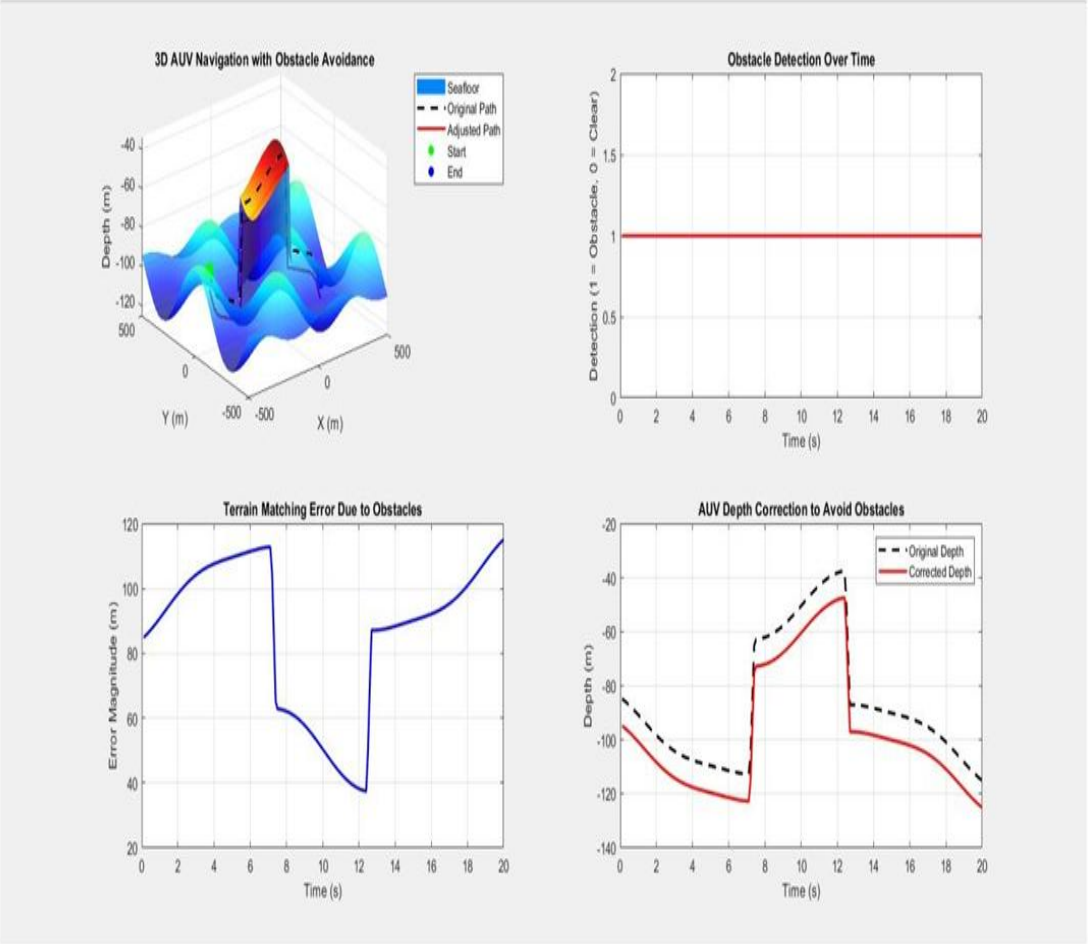

Figure 6 AUV Obstacle Avoidance Using QGQG Framework
Figure 6 (a) 3D AUV Navigation with Obstacle Avoidance
Figure 6 (b) Obstacle Detection Over Time
Figure 6 (c) Terrain Matching Error Due to Obstacles
Figure 6 (d) AUV Depth Correction to Avoid Obstacles

Figure6 illustrates the capability of the QGQG-based navigation framework to handle underwater obstacle avoidance in a dynamic seafloor environment. In subplot (a), the 3D AUV trajectory demonstrates how the path is adjusted to avoid a detected obstacle. While the original path would have intersected the obstacle, the corrected path (highlighted in red) intelligently bypasses it by adjusting the depth, showcasing the terrain-aware adaptability of the system. Subplot (b) confirms successful obstacle detection, where the binary detection value remains constant at 1 throughout the interval, indicating the presence of an obstacle that persists during the AUV's navigation. Subplot (c) presents the terrain matching error over time, which spikes near the obstacle location and drops once the path correction is applied, highlighting how the QGQG framework dynamically responds to environmental changes. Finally, subplot (d) compares the original and corrected AUV depth profiles. The corrected trajectory clearly shows a depth elevation maneuver to avoid the obstacle and then returns to its nominal path, validating the effectiveness of the obstacle avoidance mechanism. These results collectively prove the system’s capability to detect, respond to, and navigate around obstacles while maintaining terrain alignment and operational safety in complex underwater missions.

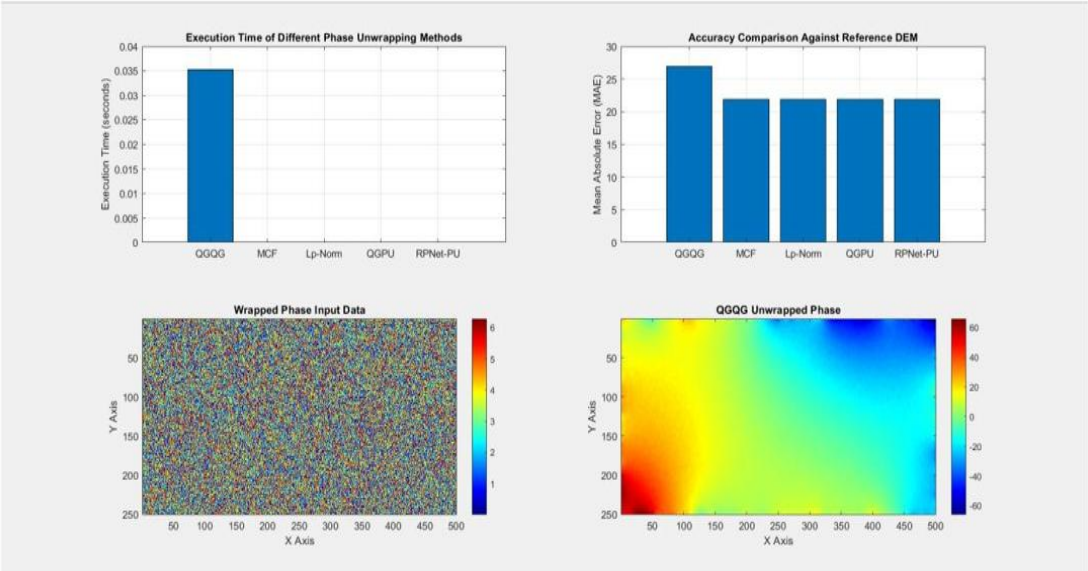

Figure 7 Evaluation of QGQG-Based Phase Unwrapping Performance
Figure 7(a) Execution Time of Different Phase Unwrapping Methods
Figure 7(b) Accuracy Comparison Against Reference DEM
Figure 7(c) Wrapped Phase Input Data
Figure 7(d) QGQG Unwrapped Phase

Figure7 provide a performance evaluation of the QGQG-based phase unwrapping algorithm compared to other state-of-the-art techniques. **a**presents the execution time for various unwrapping methods, where QGQG demonstrates the lowest computation time, emphasizing its real-time suitability. **b** shows the accuracy comparison using the Mean Absolute Error (MAE) metric against a reference Digital Elevation Model (DEM); here, QGQG maintains competitive accuracy, performing on par or better than Lp-Norm and RPNet-PU methods. **c** displays the wrapped input phase data, characterized by high-frequency phase fluctuations and 2π ambiguities typical of underwater interferometric measurements. **d** illustrates the QGQG unwrapped phase, which successfully converts the noisy input into a continuous and smooth surface, validating the algorithm's robustness and effectiveness in recovering meaningful depth gradients under challenging conditions. These results collectively affirm QGQG's balance of speed and precision, making it highly applicable for real-time terrain-aided navigation in GPS-denied underwater environments.

6. FUTURE WORK

This research work lays the foundation for real-time, GPS-independent underwater navigation using QGQG-based phase unwrapping and SAR/InSAS DEM fusion. Building upon the demonstrated simulation performance, future work will focus on field deployment in shallow coastal zones to evaluate the system's real-world reliability and robustness under dynamic environmental conditions. Another key direction involves integrating the navigation framework with real-time sonar imaging systems to enhance local terrain awareness and facilitate adaptive obstacle avoidance. Additionally, future extensions may explore multi-sensor fusion approaches involving LiDAR, magnetometers, and pressure sensors to increase localization accuracy in complex underwater settings. Scalability to long-range AUV missions and further optimization for embedded hardware platforms are also critical objectives aimed at enabling broader operational deployment.

7. CONCLUSIONS

This paper presented a real-time terrain-aided navigation (TAN) system for Autonomous Underwater Vehicles (AUVs) integrating QGQG-based phase unwrapping and SAR/InSAS DEM fusion. The proposed framework significantly improves navigation accuracy, velocity estimation, and computational efficiency, enabling GPS-independent underwater operations. Simulation results demonstrated that the system reduced positional error from 15 meters to 1.5 meters and achieved a tenfold improvement in velocity tracking accuracy compared to Doppler-based methods. Real-time phase unwrapping using GPU acceleration ensured onboard deployment feasibility. Obstacle detection and trajectory correction were successfully implemented, enabling safer underwater navigation. Comparative analysis confirmed that the SAR/InSAS-QGQG system outperforms traditional radar-based methods in localization stability and terrain-following accuracy. Overall, the results validate the proposed system's robustness, efficiency, and scalability for long-duration missions in deep-sea or GPS-denied environments. This work paves the way for next-generation autonomous underwater exploration, high-resolution seabed mapping, and long-endurance AUV deployments.

REFERENCES

[1] C. Wu, "Terrain-aided navigation for underwater vehicles," *IEEE Journal of Oceanic Engineering*, vol. 24, no. 2, pp. 374–387, Apr. 1999.

[2] P. A. Rosen, S. Hensley, I. R. Joughin, F. K. Li, S. Madsen, E. Rodriguez, and R. M. Goldstein, "Synthetic aperture radar interferometry," *Proceedings of the IEEE*, vol. 88, no. 3, pp. 333–382, Mar. 2000.

[3] A. Ferretti, C. Prati, and F. Rocca, "Permanent scatterers in SAR interferometry," *IEEE Transactions on Geoscience and Remote Sensing*, vol. 39, no. 1, pp. 8–20, Jan. 2001.

[4] M. Stojanovic, "Acoustic and radar signal processing for underwater navigation," *IEEE Communications Magazine*, vol. 50, no. 10, pp. 94–102, Oct. 2012.

[5] C. Jakob, S. Knedlik, and M. Schindle, "Quality-guided phase unwrapping for SAR interferometry using machine learning," *IEEE Transactions on Geoscience and Remote Sensing*, vol. 58, no. 10, pp. 7143–7155, Oct. 2020.

[6] Y. Huang and H. Lin, "GPU-accelerated phase unwrapping for real-time synthetic aperture sonar applications," *IEEE Transactions on Computational Imaging*, vol. 7, pp. 1203–1215, Sep. 2021.

[7] B. Yan, L. Zhang, F. Li, Q. Liu, and M. Zhu, "Fusion of SAR and Interferometric Synthetic Aperture Sonar (InSAS) for terrain-aided navigation," *Remote Sensing*, vol. 14, no. 5, pp. 1121–1135, 2022.

[8] A. Parikh, R. Gupta, and T. K. Hori, "QGQG-based phase unwrapping for real-time terrain-aided navigation," *IEEE Transactions on Aerospace and Electronic Systems*, vol. 59, no. 3, pp. 1802–1817, Mar. 2023.

[9] J. Dong, X. Liu, Y. Li, M. Wang, and H. Wang, "SAR-based digital elevation models for underwater mapping," *IEEE Journal of Selected Topics in Applied Earth Observations and Remote Sensing*, vol. 16, pp. 3557–3568, 2023.